Bilge Uluslararası Fen ve Teknoloji Araştırmaları Dergisi
Bilge International Journal of Science and Technology Research
1(1), 9-15, 2017

Structural and Spectroscopic (FT-IR and NMR) Analyses on (*E*)-pent-2-enoic Acid

Nuri ÖZTÜRK[1], Halil GÖKCE[2*]

[1]Giresun University, Dereli Vocational School, 28950, Giresun, Turkey
[2]Giresun University, Vocational School of Health Services, 28200, Giresun, Turkey

* Corresponding author (İletişim yazarı): * halil.gokce@giresun.edu.tr

Abstract: Proton and carbon-13 NMR chemical shifts and vibrational frequencies (FT-IR) of *trans*-2-pentenoic acid (2-pentenoic acid or (*E*)-pent-2-enoic acid) were studied, both experimentally and theoretically. The optimized molecular geometric parameters of monomer and dimer forms, vibrational frequencies and NMR chemical shifts of the mentioned compound were computed by using DFT/B3LYP/6-311+G(2d,p) level. The computed data were compared with experimental ones. The HOMO and LUMO analyses were performed at the mentioned computational level.

Keywords: *trans*-2-pentenoic acid, 2-pentenoic acid, (*E*)-pent-2-enoic acid), FT-IR spectroscopy, DFT/B3LYP, ^{1}H and ^{13}C NMR chemical shifts, HOMO-LUMO.

1. Introduction

Unsaturated fatty acids are very important compounds in food, nutrition and health sciences due to their role in biological processes especially for humans. These acids can be classified as monounsaturated fatty acids, polyunsaturated fatty acids and acetylenic fatty acids. They can be found in trans or cis molecular forms, which exhibit long nonpolar unsaturated alkyl chains and polar carboxylic head groups (Sonnect et al., 2015). An experimental study on α,β-unsaturated carboxylic acid (2-methyl-2-pentenoic acid) was performed by using in situ attenuated total reflection infrared (ATR-IR) spectroscopic tecknique (Tan and Williams, 2013).

Quantum chemical computation methods have been widely used to investigate structural, spectroscopic, electronic, magnetic, nonlinear optical and thermodynamic properties of molecules. Density functional theory (DFT) method has been used in many studies in the literature for effective and accuracy evaluation of molecular properties (Gökce and Bahçeli, 2013; Akyıldırım et al., 2017). The aim of this study is to investigate molecular structures for monomeric and dimeric, vibrational wavenumebers, ^{1}H and ^{13}C NMR chemical shifts and HOMO-LUMO properties of 3 *trans*-2-pentenoic acid (2-pentenoic acid or (*E*)-pent-2-enoic acid) molecule, both experimentally (FT-IR and NMR) and theoretically (DFT/B3LYP/6-311+G(2d,p) level).

2. Computational Details

All calculations were performed by using Gaussian 09W program and the computed results were visualized with GaussView5 program (Frisch et al., 2009; Dennington et al., 2009). The optimized molecular geometric parameters for monomeric and dimeric forms, vibrational wavenumbers, proton and carbon-13 NMR chemical shifts and HOMO-LUMO analyses of the title molecule were computed by using DFT (Density Functional Theory)/B3LYP (Becke's three parameters exact exchange-functional (B3) combined with gradient-corrected correlational functional of Lee, Yang, Parr (LYP)) method with 6-311+G(2d,p) basis set. (Lee et al., 1988; Becke, 1993). The calculated vibrational wavenumbers were scaled with 0.954 (in the region of 1600-4000 cm^{-1}) and 0.989 (in the region of 0-1600 cm^{-1}) for B3LYP/6-311+G(2d,p) level (Wang et al., 2015). The vibrational frequency assignments were performed by using VEDA 4 program in terms of potential energy distribution (PED) (Jamr'oz, 2004). For NMR chemical shift computations, the optimized molecular structures in chloroform of monomer and dimer forms of the title molecule were first obtained at B3LYP/6-311+G(2d,p) level by using integral equation formalism polarizable continuum model (IEFPCM) method. Then, proton and carbon-13 NMR chemical shifts were calculated with the mentioned computational level in chloroform by using gauge invariant atomic orbital (GIAO) method (London, 1937; Ditchfield, 1974; Wolinski et al., 1990). Additionally, HOMO and LUMO energy values and their shapes were calculated with B3LYP/6-311+G(2d,p) level in gas phase of the title molecule.

3. Results and Discussion

3.1. Molecular structure

The optimized molecular structures of monomeric and dimeric forms of *trans*-2-pentenoic acid (2-pentenoic acid or (*E*)-pent-2-enoic acid) molecule were given in Fig. 1. The experimental (single-crystal X-ray study) (Peppel et al., 2015) and calculated (with B3LYP/6-311+G(2d,p) level) structural parameters for monomeric and dimeric forms of the title molecule were summarized in Table 1.

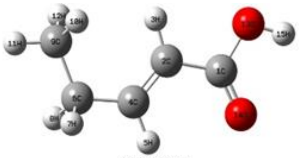

(a) Monomer

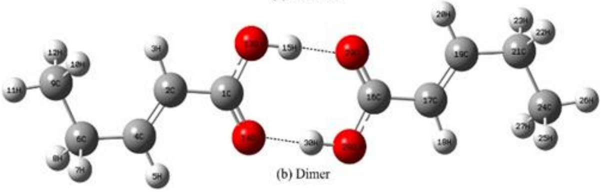

(b) Dimer

Figure 1. The optimized (a) monomeric and (b) dimeric molecular structures of (*E*)-pent-2-enoic acid.

As can be seen from results in Table 1, *trans*-2-pentenoic acid (2-pentenoic acid or (*E*)-pent-2-enoic acid) molecule may be existed in dimeric form by via strong inter-molecular hyrogen bonds in solid phase. Especially, the C1=O14 and C1-O13 bond lengths were computed as 1.2088 Å and 1.3606 Å in monoric form, whereas they were calculated 1.2305 Å and 1.3226 Å in dimeric form, respectively. The experimental values for these bond lengths were recorded as 1.2337(14) Å and 1.3223(13) Å, respectively (Peppel et al., 2015). Similarly, inter-molecular hydrogen bond parameters (H15···O29, O13···O29 and O13-H15···O29) in dimeric form of the title molecule were experimentally found as 1.69(2) Å, 2.6322(13) Å and 173.3(19)°, respectively (Peppel et al., 2015). These parameters were calculated 1.6407 Å, 2.6448 Å and 178.82°, respectively. The O13-H15 bond length was recorded as 0.95(2)/0.9697/1.0042 Å (exp./cal. for monomer/cal. for dimer) (Peppel et al., 2015).

Table 1. Experimental and calculated bond lengths and bond angles of (*E*)-pent-2-enoic acid.

Bond lengths (Å)	X-Ray[a]	Calculated		Bond angles (°)	X-Ray[a]	Calculated	
		Monomer	Dimer			Monomer	Dimer
C1-C2	1.4723(16)	1.4747	1.4742	C2-C1-O13	113.26(10)	111.32	112.87
C1-O13	1.3223(13)	1.3606	1.3226	C2-C1-O14	123.99(10)	126.75	123.65
C1=O14	1.2337(14)	1.2088	1.2305	C13-C1-O14	122.75(11)	121.94	123.48
C2-H3	0.9500	1.0822	1.0822	C1-C2-H3	119.0	116.66	115.98
C2=C4	1.3301(16)	1.3334	1.3334	C1-C2-C4	122.06(10)	120.61	121.24
C4-H5	0.9500	1.0874	1.0872	H3-C2-C4	119.0	122.74	122.78
C4-C6	1.4981(16)	1.4957	1.4960	C2-C4-H5	117.2	116.98	117.04
C6-H7	0.9900	1.0977	1.0978	C2-C4-C6	125.63(10)	126.83	126.79
C6-H8	0.9900	1.0977	1.0978	H5-C4-C6	117.2	116.19	116.17
C6-C9	1.5239(16)	1.5265	1.5264	C4-C6-H7	108.4	107.58	107.58
C9-H10	0.9800	1.0924	1.0924	C4-C6-H8	108.4	107.58	107.58
C9-H11	0.9800	1.0915	1.0915	C4-C6-C9	115.33(10)	116.59	116.59
C9-H12	0.9800	1.0924	1.0924	H7-C6-H8	107.5	104.40	104.40
O13-H15	0.95(2)	0.9697	1.0042	H7-C6-C9	108.4	109.98	109.98
H15···O29	1.69(2)	-	1.6407	H8-C6-C9	108.4	109.98	109.98
O13···O29	2.6322(13)	-	2.6448	C6-C9-H10	109.5	111.48	111.50
				C6-C9-H11	109.5	110.41	110.41
				C6-C9-H12	109.5	111.48	111.50
				H10-C9-H11	109.5	107.70	107.70
				H10-C9-H12	109.5	107.91	107.88
				H11-C9-H12	109.5	107.70	107.70
				C1-O13-H15	108.7(12)	106.45	110.49
				O13-H15···O29	173.3(19)	-	178.82

[a] Taken from (Peppel et al., 2015)

The C2=C4 bond length was found as 1.3301(16) Å (exp.) and 1.3334 Å (for both monomer and dimer) (cal.). The C1-C2, C4-C6 and C6-C9 bond lengths were calculated as 1.4747/1.4742 Å, 1.4957/1.4960 Å and 1.5265/1.5264 Å, while they were experimetally recorded as 1.4723(16) Å, 1.4981(16) Å and 1.5239(16) Å, respectively (Peppel et al., 2015).

3.2. Vibrational frequencies

There are 15 atoms and 39 fundamental vibrational modes of *trans*-2-pentenoic acid (2-pentenoic acid or (*E*)-pent-2-enoic acid) molecule. The molecule belongs to C_s point group and all vibrational modes are active under C_s symmetry. The 39 vibrational modes were distributed as 25A′+14A″. The experimental (recorded in liquid form) (AIST, 2017) and calculated vibrational wavenumbers, IR intensities, vibrational assignments and symmetry species of the title molecule were listed in Table 2. The vibrational wavenumbers for monomeric and dimeric forms of the title molecule were computed at B3LYP/6-311+G(2d,p) level. The experimental (AIST, 2017) and simulated IR spectra of the title molecule are given in Fig. 2.

Table 2. Experimental and calculated vibrational wavenumbers and their assignments of (*E*)-pent-2-enoic acid.

Sym.	Assignments (PED%)	Exp. freq.	DFT/B3LYP/6-311+G(2d,p) level		
		IR (cm^{-1})	Unscaled freq.	Scaled freq.	I_{IR}
A″	$\tau O_{13}C_1C_2C_4(60)+\tau C_9C_6C_4C_2(29)$	-	67	66	1.887
A″	$\tau C_1C_2C_4C_6(58)+\tau O_{13}C_1C_2C_4(19)+\tau C_9C_6C_4C_2(11)$	-	145	143	1.051
A′	$\delta C_6C_4C_2(38)+\delta C_1C_2C_4(36)+\delta O_{13}C_1C_2(12)+\delta C_9C_6C_4(11)$	-	146	144	0.498
A″	$\rho CH_3(36)+\tau C_1C_2C_4C_6(28)+\tau C_9C_6C_4C_2(12)+\tau HCCC(11)$	-	201	199	0.151
A′	$\delta C_9C_6C_4(34)+\delta C_1C_2C_4(25)+\delta O_{13}C_1C_2(12)+\delta C_6C_4C_2(10)$	-	258	256	2.282
A″	$\rho CH_3(66)+\tau C_9C_6C_4C_2(13)+\tau C_1C_2C_4C_6(10)$	-	282	278	0.768
A′	$\delta O_{13}C_1C_2(44)+\delta OCO(12)+\nu C_1C_2(12)+\delta C_1C_2C_4(10)$	483	457	452	12.044
A′	$\delta C_9C_6C_4(33)+\delta C_6C_4C_2(20)+\delta O_{13}C_1C_2(18)$	540	534	528	0.958
A″	$\tau HOCC(84)$	-	580	574	63.849
A′	$\delta OCO(53)+\nu CO(16)$	-	658	651	39.226
A″	$\gamma O_{14}C_2O_{13}C_1(29)+\rho CH_2(27)+\tau HOCC(14)+\tau HCCC(14)$	697	693	685	49.595
A″	$\gamma O_{14}C_2O_{13}C_1(43)+\rho CH_2(19)$	787	788	779	6.280
A′	$\nu C_9C_6(48)+\nu C_6C_4(32)$	865	887	877	19.577
A″	$\tau HCCC(56)+\gamma O_{14}C_2O_{13}C_1(15)$	891	890	881	17.401
A′	$\nu C_1C_2(41)+\nu CO(12)$	933	943	933	1.775
A″	$\tau HCCC(87)$	980	1018	1007	26.720
A′	$wCH_2(23)+\nu C_6C_4(20)+\rho CH_3(13)+\nu C_9C_6(10)$	1025	1042	1031	29.156
A′	$\nu C_9C_6(24)+\rho CH_3(13)$	1079	1099	1087	89.035
A″	$\tau C_9C_6C_4C_2(24)+tCH_2(24)+\rho CH_3(11)$	1073	1111	1099	2.379
A′	$\nu CO(36)+\delta HOC(22)$	1130	1148	1136	276.945
A′	$\delta HCC(40)+\delta HOC(32)$	1268	1281	1267	19.650
A″	$tCH_2(62)+\rho CH_3(15)$	1288	1292	1278	0.304
A′	$\delta HCC(67)+\nu C{=}C(12)$	1334	1333	1318	29.169
A′	$\delta HOC(17)+\delta HCC(12)+wCH_2(11)$	-	1369	1353	58.574
A′	$wCH_2(31)+\delta_s CH_3(17)$ (sym. bend.)	1384	1391	1376	16.827
A′	$\delta_s CH_3(82)$ (sym. bend.)	1420	1419	1403	13.017
A′	$\delta_s CH_2(87)$	-	1463	1447	26.390
A″	$\delta_s CH_3(85)$	-	1501	1484	8.676
A′	$\delta_s CH_3(75)$	1496	1509	1492	3.467
A′	$\nu C{=}C(64)+\delta HCC(17)$	1653	1698	1620	162.307
A′	$\nu C{=}O(79)$	1697	1781	1699	293.639
A′	$\nu_s CH_2(99)$	2883	2998	2860	16.449
A″	$\nu_{as} CH_2(98)$	-	3011	2872	8.444
A′	$\nu_s CH_3(99)$	-	3031	2892	19.949
A″	$\nu_{as} CH_3(94)$	2940	3091	2949	26.171
A′	$\nu_{as} CH_3(87)$	2973	3095	2953	27.223

A′	νC_4H_5(100)	-	3142	2997	2.265
A′	νC_2H_3(100)	-	3194	3047	3.303
A′	νOH(100)	2500-3500	3759	3586	85.703
ν, stretching; δ, in-plane bending; τ, torsion; γ, out-of-plane bending; δ_s, scissoring and symmetric bending; w, wagging; t, twisting; ρ, rocking; Sym., symmetry species; I_{IR}, IR intensity (km/mol); PED, potential energy distribution.					

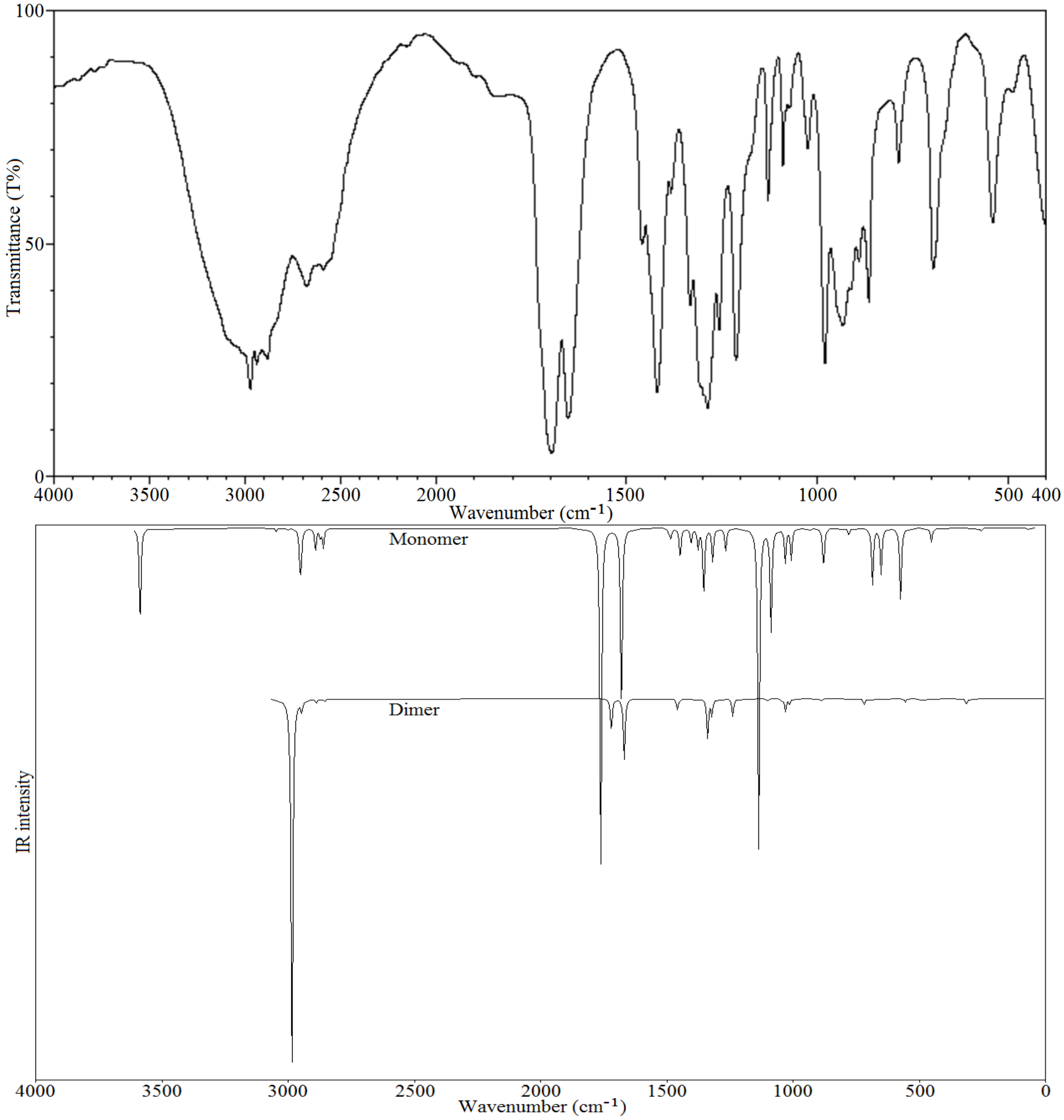

Figure 2. Experimental (top) and simulated (bottom) IR spectra of or (*E*)-pent-2-enoic acid.

FT-IR spectrum in dimeric carboxylic acids give a very broad band in the region of 2500-3300 cm^{-1} due to OH vibrational streching band (Colthup et al., 1964; Bellamy, 1975; Lambert et al., 1987; Silverstein and Webster, 1998; Stuart, 2004). The observed band in the region of 2500-3500 cm^{-1} in Fig. 2 can be indicated to dimeric form of the title molecule. This band was computed at 3586 cm^{-1} for monomer, whereas it was calculated at 2990 and 2888 cm^{-1} for dimer. The OH in-plane bending modes can be appeared as mixed with other vibrational modes in the region of 1200-1450 cm^{-1} (Colthup et al., 1964; Bellamy, 1975; Lambert et al., 1987; Silverstein and Webster, 1998; Stuart, 2004). For monomeric form, the OH in-plane bending modes were recorded at 1130 and 1268 cm^{-1} (AIST, 2017) and they were calculated at 1136, 1267 and 1353 cm^{-1}. For dimeric form, the OH in-plane bending modes were computed at 1478, 1455, 1334 and 1329 cm^{-1}. Similarly, the OH out-of-plane bending mode for monomeric form was obtained at 697 (exp.)/685 (cal. with 17% contribution of PED) and 580 (cal. with PED contribution of 84%) cm^{-1}, whereas this band for dimeric form was calculated at 975 and 1024 cm^{-1}.

The position of this stretching band can be changed depending on effects such as the physical state, electronic and mass effects of neighboring substituents, conjugations and inter- and intar-molecular hydrogen bonding (Colthup et al., 1964; Bellamy, 1975; Lambert et al., 1987; Silverstein and Webster, 1998; Stuart, 2004). The C=O stretching band was recorded at 1697 cm^{-1} as a strong (AIST, 2017) and it was computed at 1699 cm^{-1} (with PED contribution of 79%) for monomer form of the title molecule. This band in dimer form was calculated at 1657, 1607 and 1592 cm^{-1}. Silverstein and Webster (Silverstein and Webster, 1998) assigned CO stretching mode in the region of 1320-1210 cm^{-1} for dimer carboxyl compounds. The CO stretching modes for dimeric form were computed at 1226, 1234, 1334 and 1329 cm^{-1}. However, this band for monomeric structure was found 1130 (exp.)/1136 (cal. with 36% contribution of PED) (AIST, 2017). The experintal and computed wavenumber values for the C=C stretching band were found at 1653 and 1620 cm^{-1} (with PED contribution of 64%).

The vibrational assignments and wavenumbers (both experimental and calculated) for other modes were given in Table 2.

3.3. ^{13}C and ^{1}H NMR chemical shift analyses

The proton and carbon-13 NMR chemical shifts for monomeric and dimeric forms of the title molecule were calculated at B3LYP/6-311+G(2d,p) level in chloroform. The experimental (Peppel et al., 2015; AIST, 2017) and computed ^{1}H and ^{13}C NMR chemical shifts were summarized in Table 3.

Table 3. Experimental and calculated proton and carbon-13 NMR chemical shifts (with recpect to TMS, all values in ppm) of (*E*)-pent-2-enoic acid.

Atoms	$\delta_{exp.}$ (chloroform-d)[a]	$\delta_{exp.}$ (chloroform-d)[b]	Monomer	Dimer
			$\delta_{cal.}$ (chloroform)	$\delta_{cal.}$ (chloroform)
C1	172.66	172.69	173.324	180.516
C2	120.02	119.76	118.994	121.208
C4	153.68	153.77	165.954	166.052
C6	25.52	25.54	29.648	29.542
C9	12.05	21.10	9.479	9.511
H3	5.83	5.82	6.014	5.977
H5	7.14	7.14	7.896	7.946
H7	2.29	2.21-2.30	2.452	2.455
H8			2.452	2.455
H10	1.09	1.08	1.014	1.028
H11			1.120	1.116
H12			1.014	1.028
H15	11.99	12.35	5.815	13.570

[a] AIST, 2017
[b] Peppel et al., 2015

Due to the highly electronegative O atom, the carboxylic acid and their derivatives occur carbon-13 NMR signal at the interval 160-180 ppm (Pavia et al., 2009). The carbon-13 NMR chemical shift signal recorded at 172.66/172.69 ppm can be assigned to C1 atom in carboxyl group of the title molecule (Peppel et al., 2015; AIST, 2017). The computed value for this carbon atom was computed at 173.324 ppm for monomer form and 180.516 ppm for dimer one. Alkene carbons generally appear between 100 ppm and 140 ppm in ^{13}C NMR chemical shift spectrum (Pavia et al., 2009). However, this chemical shift region can be changed due to other groups (methylene, methyl, etc.) bonded to alkene carbons. The experimental and computed NMR signals for C2 and C4 atoms were found at 120.02 (exp.)/119.79 (exp.)/118.994 (cal. for monomer)/121.208 (cal. for dimer) ppm and 153.68 (exp.)/153.77 (exp.)/165.954 (cal. for monomer)/166.052 (cal. for dimer) ppm, respectively (Pavia et al., 2009). The NMR signals for carbons of methylene and methyl groups were given in Table 3.

The proton NMR signal of H15 atom in carboxyl group in the title molecule were recorded at 11.99/12.35 ppm (Pavia et al., 2009), while the calculated value for this proton were at 5.815/13.570 ppm (monomer/dimer). The NMR signals obtained for H3 and H5 proton atoms are at 5.83 (exp.)/5.82 (exp.)/6.014 (cal. for monomer)/5.977 (cal. for dimer) ppm and 7.14 (exp.)/7.14 (exp.)/7.896 (cal. for monomer)/7.949 (cal. for dimer) ppm, respectively (Pavia et al., 2009). The methylene protons (H7 and H8) were given rise to resonance signals at 2.29 (exp.)/2.21-2.30 (exp.)/2.452 (cal. for monomer)/2.455 (cal. for dimer) ppm, while the methyl protons (H10, H11 and H12) were found at 1.09 (exp.)/1.08 (exp.)/1.014-1.020 (cal. for monomer)/1.028-1.116 (cal. for dimer) ppm (Pavia et al., 2009).

3.4. HOMO and LUMO analyses

The highest occupied molecular orbital (HOMO) and lowest unoccupied molecular orbital (LUMO) are called as frontier molecule orbitals (FMOs). They are main orbitals taking part in chemical reaction (Fukui, 1982). The HOMO presents the outermost orbital filled by electrons. It is directly related to the ionization potential. Behaving as an electron donor, it can be considered as valance band. The LUMO implies the first empty innermost orbital unfilled by electrons. It is directly related to the electron affinity. Behaving as an electron acceptor, it can be thought as conductance band.

The HOMO-LUMO energy band gap is an indicatator of molecular chemical stability and it is a very important parameter for determination of molecular electrical properties (Pearson, 1986). The HOMO and LUMO energy values, their shapes and energy gap were depicted in Fig. 3. As seen from Fig. 3, HOMO is localized on other groups excluding methyl and OH groups, while the LUMO is placed over whole molecule expecting methyl group. The HOMO and LUMO energy values were computed as -7.680 eV and -1.492 eV, respectively. Similarly, HOMO-LUMO energy band gap was obtained as 6.188 eV.

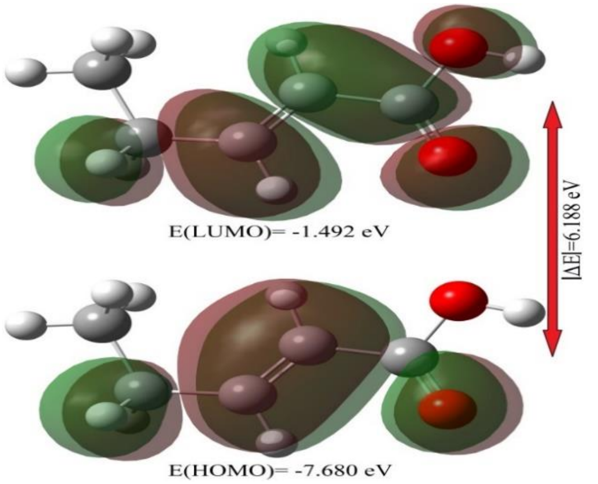

Figure 3. Simulated HOMO and LUMO shapes of (*E*)-pent-2-enoic acid.

4. Conclusion

The experimental spectroscopic analyses of *trans*-2-pentenoic acid (2-pentenoic acid or (*E*)-pent-2-enoic acid) were studied by using FT-IR and NMR methods. Quantum chemical computations were performed with DFT/B3LYP/6-311+G(2d,p) level. The observed broad band in the region of 2500-3300 cm^{-1} in FT-IR spectrum and signal at 11.99/12.35 ppm in proton NMR chemical shifts are indicated to dimeric form of the title molecule. The experimental values are in a good aggrement with computed data.

References

AIST, (2017). National Institute of Advanced Industrial Science and Technology Spectral Database for Organic Compounds, SDBS. http://sdbs.db.aist.go.jp/sdbs/cgi-bin/cre_index.cgi, (Accessed on 10 March 2017).

Akyıldırım, O., Gökce, H., Bahçeli, S., Yüksek, H. (2017). Theoretical and Spectroscopic (FT-IR, NMR and UV-Vis.) Characterizations of 3-p-chlorobenzyl-4-(4-carboxybenzylidenamino)-4,5-dihydro-1H-1,2,4-triazol-5-one Molecule. Journal of Molecular Structure, 1127: 114-123.

Becke, A.D. (1993). Density-functional Thermochemistry. III. The Role of Exact Exchange. The Journal of Chemical Physics, 98: 5648-5652.

Bellamy, L.J. (1975). The Infrared Spectra of Complex Molecules, 3rd ed. Wiley, New York.

Colthup, N.B., Daly, L.H., Wiberley, E. (1964). Introduction to Infrared and Raman Spectroscopy, Academic Press, New York.

Dennington, R., Keith, T., Millam J. (Eds.) (2009). GaussView, Version 5, Semichem Inc., Shawnee Mission KS.

Ditchfield, R. (1974). Self-consistent Perturbation Theory of Diamagnetism. Molecular Physics, 27: 789-807.

Frisch, M.J., Trucks, G.W., Schlegel, H.B., Scuseria, G.E., Robb, M.A., Cheeseman, J.R., Scalmani, G., Barone, V., Mennucci, B., Petersson, G.A., Nakatsuji, H., Caricato, M., Li, X., Hratchian, H.P., Izmaylov, A.F., Bloino, J., Zheng, G., Sonnenberg, J.L., Hada, M., Ehara, M., Toyota, K., Fukuda, R., Hasegawa, J., Ishida, M., Nakajima, T., Honda, Y., Kitao, O., Nakai, H., Vreven, T., Montgomery Jr., J.A., Peralta, J.E., Ogliaro, F., Bearpark, M., Heyd, J.J., Brothers, E., Kudin, K.N., Staroverov, V.N., Kobayashi, R., Normand, J., Raghavachari, K., Rendell, A., Burant, J.C., Iyengar, S.S., Tomasi, J., Cossi, M., Rega, N., Millam, J.M., Klene, M., Knox, J.E., Cross, J.B., Bakken, V., Adamo, C., Jaramillo, J., Gomperts, R., Stratmann, R.E., Yazyev, O., Austin, A.J., Cammi, R., Pomelli, C., Ochterski, J.W., Martin, R.L., Morokuma, K., Zakrzewski, V.G., Voth, G.A., Salvador, P., Dannenberg, J.J., Dapprich, S., Daniels, A.D., Farkas, Ö., Foresman, J.B., Ortiz, J.V., Cioslowski, J., Fox, D.J. (2009). Gaussian 09, Revision C.01, Gaussian, Inc., Wallingford CT.

Fukui, K. (1982). Role of Frontier Orbitals in Chemical Reactions. Science, 218: 747-754.

Gökce, H., Bahçeli, S. (2013). Molecular Structure, spectroscopic properties and DFT calculations of 2-(methylthio)nicotinic acid. Optics and Spectroscopy, 115(4): 469–483.

Jamr'oz, M.H. (2004). Vibrational Energy Distribution Analysis, VEDA4, Warsaw.

Lambert, J.B., Shurvell, H.F., Cooks, R.G. (1987). Introduction to Organic Spectroscopy, Macmillan Publish, NewYork, USA.

Lee, C., Yang, W., Parr, R.G. (1988). Development of the Colle-Salvetti Correlation-Energy Formula into a Functional of the Electron Density. Physical Review B, 37: 785-789.

London, F. (1937). Théorie Quantique Des Courants Interatomiques Dans Les Combinaisons Aromatiques. Journal de Physique et le Radium, 8: 397-409.

Pavia, D.L., Lampman, G.M., Kriz, G.S., Vyvyan, J.R. (2009). Introduction to Spectroscopy, Brooks/Cole Cengage Learning, USA.

Pearson, R.G. (1986). Absolute Electronegativity and Hardness Correlated with Molecular Orbital Theory. Proceedings of the National Academy of Sciences of the United States of America, 83: 8440-8441.

Peppel, T., Sonneck, M., Spannenberg, A., Wohlrab, S. (2015). Crystal Structure of (E)-pent-2-enoic Acid. Acta Crystallographica E71: o316.

Silverstein, R.M., Webster, F.X. (1998). Spectroscopic Identification of Organic Compound, 6nd ed. John Willey & Sons, New York.

Sonneck, M., Peppel, T., Spannenberg, A., Wohlrab, S. (2015). Synthesis and Molecular Structures of (E)-non-2-enoic Acid and (E)-dec-2-enoic Acid. Crystals, 5(4): 466-474.

Stuart, B.H. (2004). Infrared Spectroscopy: Fundamentals and Applications, JohnWilley & Sons, England.

Tan, S., Williams, C.T. (2013). An In Situ Spectroscopic Study of Prochiral Reactant–Chiral Modifier Interactions on Palladium Catalyst: Case of Alkenoic Acid and Cinchonidine in Various Solvents. J. Phys. Chem. C, 117(35): 18043–18052.

Wang, Z., Chen, J., Li, L., Zhou, Z., Geng, Y., Sun, T. (2015). Detailed Structural Study of β-artemether: Density Functional Theory (DFT) Calculations of Infrared, Raman Spectroscopy, and Vibrational Circular Dichroism. Journal of Molecular Structure, 1097: 61-68.

Wolinski, K., Himton, J.F., Pulay, P. (1990). Efficient implementation of the gauge-independent atomic orbital method for NMR chemical shift calculations. Journal of the American Chemical Society, 112: 8251-8260.